Growth and experimental evidences for doped nanofilms by X-ray photoemission spectroscopy data analyses

A. Hamodi[1,3], Tuncer Hökelek[1], Natheer B. Mahmood[2], Y. I. Hamodi[3], T.Bdair[4], A.T. Salih[5] & K. K. Naji[2,6]

[1] Department of Physics, Hacettepe University, 06800 Beytepe-Ankara, Turkey.
[2] Ministry of Education/General Directorate of Baghdad Education Karkh2/Iraq.
[3] Minstry of Higher Education and Scientific Research, 55509 Rusafa-Baghdad, Iraq.
[4] Department of Computer Aided Medical Procedures and Augmented Reality, Technical University of Munich, 80336 Munich, Germany.
[5] Nanotechnology and Advanced Materials Research Center, the University of Technology, 35109-Baghdad, Iraq.
[6] Lafargeholcim Company, 38070 Saint-Quentin-Fallavier, France.

arpes.antny@gmail.com

Abstract. By using the molecular beam epitaxy growth technique, the impacts of growth temperatures for Bi2Te3 thin films were investigated, besides of the substrate temperatures on growth. Moreover, the full width half maximums, based on the X-ray photoemission spectroscopy measurements, have been shown clear results for Cr-Te bonds in chromium doped Bi2Te3 thin films. The current aim is a spotlight on enlightening how chromium is joined within Bi2Te3 epitaxial thin films in the process of doping concentration by providing detailed experimental evidences through the systematic structure and electronic investigations of the compound.

1. Introduction

The three-dimensional topological insulators are known to have high modern connected materials in the memory devices environment and spintronic thermoelectric materials [1][2][3][4]. By molecular beam epitaxy process, Bi2Te3 epitaxial films are unpretentiously grown, a mechanism that appears as its limits in the volume output [5][6]. Reliance on stoichiometric configuration, the various crystal structures of bismuth tellurite phase may be possible, such as the BiTe structure forms with lower Te concentration while the , Bi3Te4 structure forms with higher Bi concentration [6][7]. The most common phase structure for bismuth tellurite is Bi2Te3. Protected by time reversal symmetry, Bi2Te3 shows conducting surface state and insulated bulk states [8][9][10], and the presence of Dirac cone at Γ point within the Brillouin zone. This system has been heavily studied by many researchers [1][11][12][13][14]. In the present work, by using MBE growth, the best substrate temperature to growth Bi2Te3 phase was reported. Moreover, a deep analysis of XPS data for Bi2Te3 and the effect of doping with different concentrations of chromium were also presented.

2. Experimental part

2.1. Growth.

In this work, Bi2Te3 samples were grown on the BaF2 substrates. By investigating the substrate temperatures for the growth, different substrate temperatures have been considered to predict the electronic structures. Moreover, the beam equivalent pressures for Bi2Te3 samples have been measured for each presented temperature in Table 1. The Bi2Te3 samples were grown by changing these parameters. Firstly, to clean the BaF2 substrate, the substrate was heated up to 350 °C for 12 minutes. Secondly, the substrate temperature is set to go down 275 °C during the MBE growth. Thirdly, the Bi2Te3 crucible is heated to 470 °C for 105 minutes. For low-temperature substrates below 275 °C, the samples show multiphase out of Bi2Te3 structure, which is the same case for high beam equivalent pressure for Bi2Te3. Fig. 1 shows x-ray photoemission (XPS) spectrum for Bi2Te3 films. For Te element, the highest core level peak, Te 3d, has been observed clearly below 700 eV and Bi 4f core level peak has been observed below 1150 eV. Fig. 2. shows ARPES measurements with high intense bulk valance bands and low intense surface state near to the Fermi edge. This result shows that the Bi2Te3 sample was successfully grown. Fig .3 shows the variation between Bi2Te3 cell and BaF2 substrate temperatures for different samples.

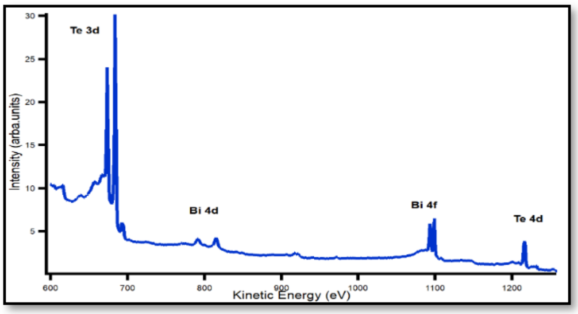

Figure 1. XPS spectrum for Bi_2Te_3 film on BaF_2 substrate using Mg K-alpha E = 1.254 Kev.

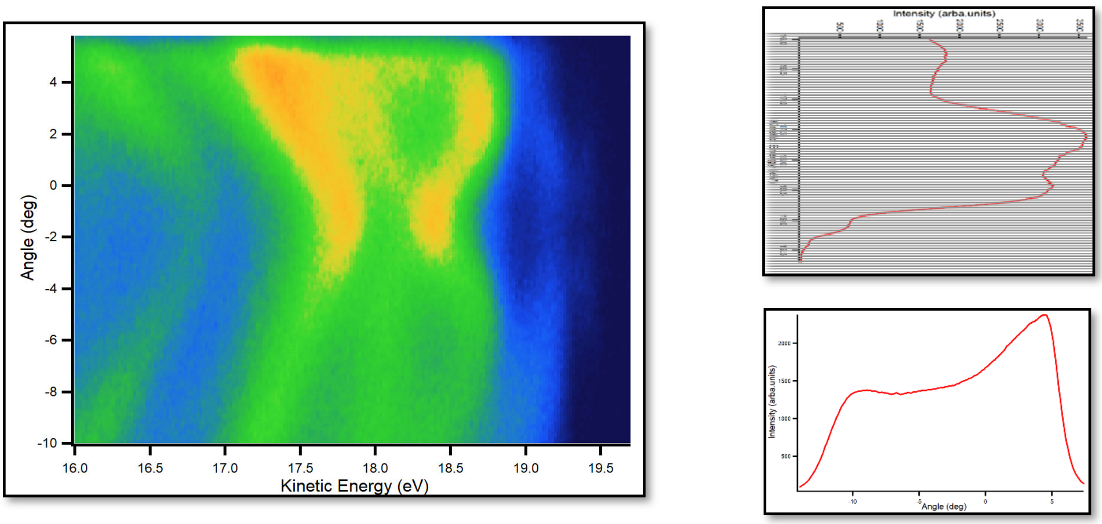

Figure 2. a) ARPES measurements of electronic bands spectrum for Bi_2Te_3 on BaF_2 substrate, measured with $hv = 21.21$ eV at 70K. (b) EDC's taken from Fig. 2a over angle (wave vector) between -10, +5.8 deg. Measured using a He Iα line of a helium plasma lamp. (c) MDCs were taken from Fig. 2a integrated over energy 16 to 19.7 eV.

Table 1. The selected temperature values of Bi_2Te_3 cell and BaF_2 substrate

BaF_2 substrate Temperature)	Bi_2Te_3 crucible Temperature	Beam equivalent pressure 10^{-7}mbar
220	435	5.83
235	450	5.32
255	520	1.30
275	470	4.76
290	550	1.22
310	470	1.70
325	310	7.50

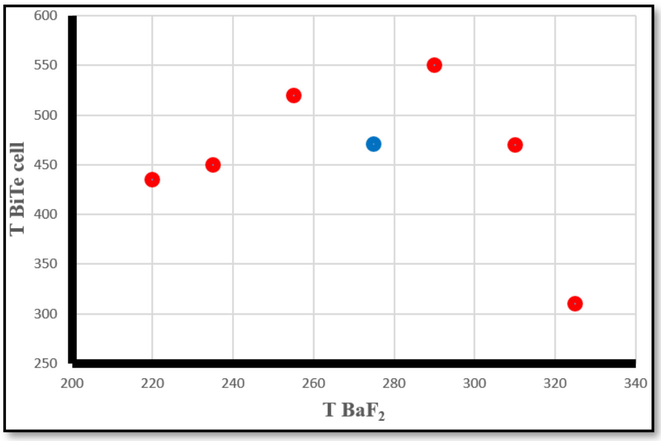

Figure 3. The temperature of Bi_2Te_3 cell vs the temperature of BaF_2 for different samples. The red dots represent unsuccessful samples. The blue dot represents a successful sample.

2.2. XPS data analysis.
With new asymmetric pseud Vogit line shape function in (Eq. 1)[15][16][17], some changes with peak shapes in Cr: BiTe samples were detected by peak asymmetry and the full width of the half maximum (FWHM). When we exchanged the new sigmoidal function (energy-related term) with ordinary FWHM in pseudo Vogit function, significant analysis of XPS data can be provided the asymmetric line shape. The variation in FWHM can have a direct effect on the line effect. For a fixed value of FWHM, the line shape will be symmetric, while for changeable FWHM, the asymmetric line shape can occur due to the difference to the peak center, with a limited area under the same curve as mentioned in fixed FWHM. The FWHM changes from 0 to 2 ω0, where w0 is the origin of the FWHM for symmetric pseudo-Voigt function [18].

$$pseudo - Voigt = (1-m)\sqrt{\frac{4\ln(2)}{\boldsymbol{\omega}_{(x)}^{2}\pi}}\,exp^{-\frac{4ln2}{\omega_x^2 2}x^2} + m\frac{\boldsymbol{\omega}_{(x)}}{2\pi\,(\boldsymbol{\omega}_{x\,/2})2+4x2} \quad \ldots Equation\ 1.$$

$$w_{(x)} = \frac{2\,w_0}{1+\exp\left(-\mathrm{a}(\mathrm{x}-\mathrm{b})\right)} \quad \ldots Equation\ 2.$$

Where x = (E - Eo), b represents the sigmoidal shift, a represents the asymmetric factor, ω0 represents the FWHM symmetry not equal to FWHM asymmetry, ω(x) is the actual FWHM of an asymmetric curve [16][17][18]. It is clear that depending on the value of m, the shapes of the peaks can be changed between Lorentzian and Gaussian shapes. XPS measurements for Bi 4f core level peaks for pure and Cr doped Bi2Te3 are shown in Fig. 4 (a) for pure Bi2Te3, (b) Crx:Bi2-xTe3 (x=0.075), (c) Crx:Bi2-xTe3 (x=0.12).

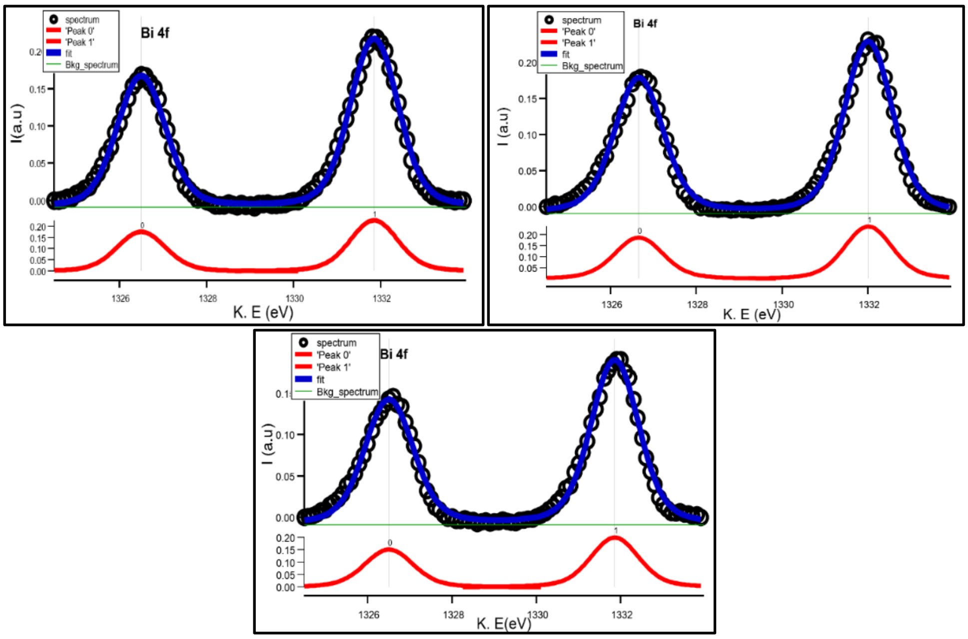

Figure 4. The Asymmetric pseud Vogit line shape function for Bi 4f core level peak for (a) Bi_2Te_3, (b) Cr_x: $Bi_{2-x}Te_3$ (x=0.075) (c) Cr_x: $Bi_{2-x}Te_3$ (x=0.12).

Asymmetric Voigt function for asymmetric peak shape shows that the asymmetries in Bi 4f core level peaks are non-detectable, despite the asymmetric factor a is greater than zero for the two doped samples, Fig. 4 b, c, the new FWHM *w(x)* does not have any change. Even though the used function was not sufficient to detect the asymmetry, the new FWHM *w(x)* was approximately constant for all Bi 4f core level peaks, which means there are no effective change in the natural line width of Bi 4f peaks (that is true if we ignore the instrumental resolution parameters in addition to the disordering on the sample surface). The splitting of spin coupling between 4f5/2 Bi and 4f7/2 Bi core level peaks was 5.4 eV.

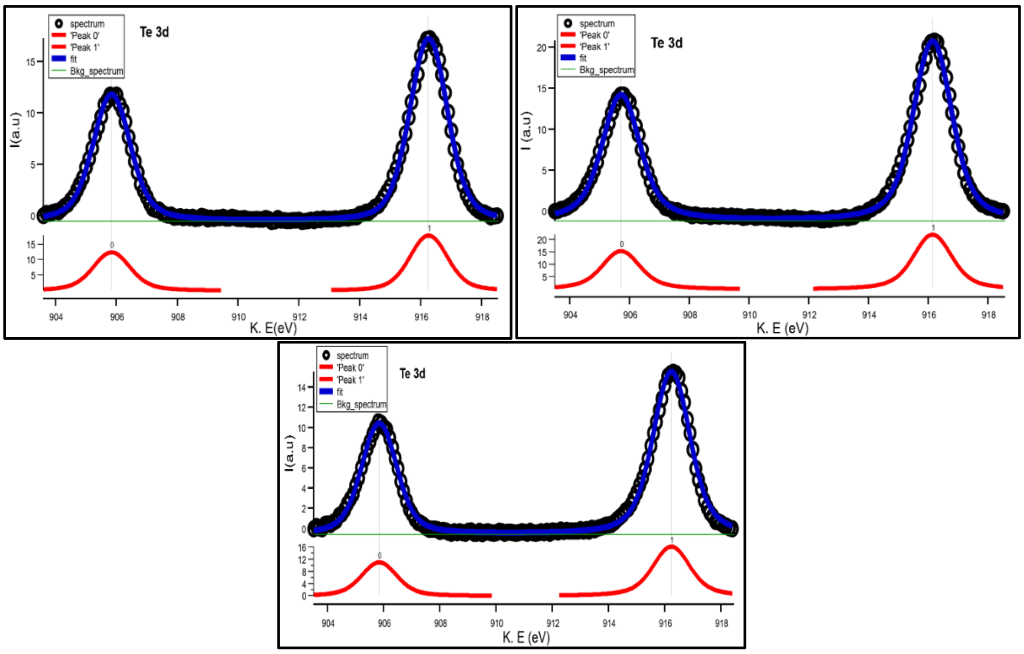

Figure 5. Asymmetric pseud Vogit line shape function for Te 3d core level peak for (a)Bi_2Te_3, (b) Cr_x:$Bi_{2-x}Te_3$ (x=0.075) (c) Cr_x:$Bi_{2-x}Te_3$ (x=0.12).

The XPS measurements for Te 3d core-level peaks are presented in Fig. 5 a-c for pure Bi_2Te_3, Cr_x:$Bi_{2-x}Te_3$ (x=0.075) and Cr_x:$Bi_{2-x}Te_3$ (x=0.12), respectively. The two peaks are emerged at specific binding energies with spin-orbital splitting approximately 10.35 eV. Even though, there was an expectation to detect the asymmetric peak line shape with a pure sample. Our result shows that the new FWHM w(x) is slightly different between the doped and non-doped samples. As we may hypothetically assumed, by ignoring the instrument effeteness on the FWHM plus the roughness on the sample surface, we claim that this slight change in FWHM comes from different bonding of Te atom with Cr and Bi atoms (see table 2). Unluckily, for our energy resolution, we are not able to confirm that the slight change is due to the above reason. For those reasons, further studies are requested.

Table 2. FWHM for core level peaks $4f_{5/2}$, $4f_{7/2}$ Bi and $3d_{3/2}$ Te, $3d_{5/2}$ Te for Bi_2Te_3, and Cr_x:$Bi_{2-x}Te_3$ (x=0.075) Cr_x:$Bi_{2-x}Te_3$ (x=0.12)

Sample	FWHM $Te3d_{3/2}$	FWHM $Te3d_{5/2}$	FWHM $Bi4f_{5/2}$	FWHM $Bi4f_{7/2}$
Bi_2Te_3	1.42	1.45	1.33	1.31
Cr_x:$Bi_{2-x}Te_3$ (x=0.075)	1.44	1.47	1.31	1.29
Cr_x:$Bi_{2-x}Te_3$ (x=0.12)	1.47	1.54	1.32	1.29

3. Conclusions

The recent study on V–VI semiconductors have shown that the 3D topological insulators are quite new scope to recognize new physics phenomena and applications. In summary, we have pointed out the convenient growth of Bi_2Te_3 thin film by the MBE method, and demonstrated the most efficient substrate temperature for the growth as well as for Bi_2Te_3 crucible. We claim that the Cr atoms may cause this change within FWHM values in 4fBi and 3dTe core-level peaks. In Particular, the presence of Cr 2p core level peaks match with Te 3d core level peaks at the same binding energy positions. Moreover, we assumed that samples with lower doping rate should present a more symmetric peak shape, due to fewer electrons in the bulk conduction band.

References

[1] Y. Xia et al., "Observation of a large-gap topological-insulator class with a single Dirac cone on the surface," Nat. Phys., vol. 5, no. 6, pp. 398–402, May 2009, doi: 10.1038/nphys1274.

[2] J. E. Moore and L. Balents, "Topological invariants of time-reversal-invariant band structures," Phys. Rev. B - Condens. Matter Mater. Phys., vol. 75, no. 12, p. 121306, Mar. 2007, doi: 10.1103/PhysRevB.75.121306.

[3] S. Selmo et al., "MOCVD growth and structural characterization of In-Sb-Te nanowires," Phys. status solidi, vol. 213, no. 2, pp. 335–338, Feb. 2016, doi: 10.1002/pssa.201532381.

[4] N. Zibouche, A. Kuc, J. Musfeldt, and T. Heine, "Transition-metal dichalcogenides for spintronic applications," Ann. Phys., vol. 526, no. 9–10, pp. 395–401, Oct. 2014, doi: 10.1002/andp.201400137.

[5] J. Kampmeier et al., "Selective area growth of Bi2Te3 and Sb2Te3 topological insulator thin films," J. Cryst. Growth, vol. 443, pp. 38–42, Jun. 2016, doi: 10.1016/j.jcrysgro.2016.03.012.

[6] F. Bonell et al., "Growth of Twin-Free and Low-Doped Topological Insulators on BaF2(111)," Cryst. Growth Des., vol. 17, no. 9, pp. 4655–4660, Sep. 2017, doi: 10.1021/acs.cgd.7b00525.

[7] A. Hamodi, T. Hökelek, Y. I. Hamodi, N. B. Mahmood, and K. K. Naji, "Electronic structure of epitaxially grown chromium-doped Bi2Te3 films," Phys. B Condens. Matter, vol. 596, p. 412413, Nov. 2020, doi: 10.1016/j.physb.2020.412413.

[8] H. Okamoto, M. E. Schlesinger, and E. M. Mueller, "Binary Alloy Phase Diagrams, 2nd Edition - ASM International," p. undefined-undefined, 2016.

[9] A. Hamodi, T. Hökelek, Y. I. Hamodi, N. B. Mahmood, and N. Nakamori, "Restorations of fresh

surfaces for topological materials by de-capping Te," Appl. Surf. Sci., vol. 530, p. 147225, Nov. 2020, doi: 10.1016/j.apsusc.2020.147225.

[10] D. Hsieh et al., "Observation of time-reversal-protected single-dirac-cone topological-insulator states in Bi2Te3 and Sb2Te3," Phys. Rev. Lett., vol. 103, no. 14, p. 146401, Sep. 2009, doi: 10.1103/PhysRevLett.103.146401.

[11] H. Zhang, C. X. Liu, X. L. Qi, X. Dai, Z. Fang, and S. C. Zhang, "Topological insulators in Bi 2 Se 3, Bi 2 Te 3 and Sb 2 Te 3 with a single Dirac cone on the surface," Nat. Phys., vol. 5, no. 6, pp. 438–442, 2009, doi: 10.1038/nphys1270.

[12] Y. L. Chen et al., "Experimental realization of a three-dimensional topological insulator, Bi2Te3," Science (80-.)., vol. 325, no. 5937, pp. 178–181, Jul. 2009, doi: 10.1126/science.1173034.

[13] M. Ahmad, K. Agarwal, and B. R. Mehta, " An anomalously high Seebeck coefficient and power factor in ultrathin Bi 2 Te 3 film: Spin–orbit interaction ," J. Appl. Phys., vol. 128, no. 3, p. 035108, Jul. 2020, doi: 10.1063/5.0007440.

[14] X. Kou and K. L. Wang, "Epitaxial Growth of Bi2X3 Topological Insulators," in Springer Series in Materials Science, vol. 285, Springer Verlag, 2019, pp. 319–349.

[15] J. Holzl, F. K. Schulte, and H. Wagner, Solid Surface Physics. Springer Berlin Heidelberg, 1979.

[16] H. P. Steinrück, T. Fuhrmann, C. Papp, B. Tränkenschuh, and R. Denecke, "A detailed analysis of vibrational excitations in x-ray photoelectron spectra of adsorbed small hydrocarbons," J. Chem. Phys., vol. 125, no. 20, p. 204706, Nov. 2006, doi: 10.1063/1.2397678.

[17] M. Schmid, H. Steinrück, and J. M. Gottfried, "A new asymmetric Pseudo-Voigt function for more efficient fitting of XPS lines," Surf. Interface Anal., vol. 47, no. 11, pp. 1080–1080, Nov. 2015, doi: 10.1002/sia.5847.

[18] J. Walton, P. Wincott, and N. Fairley, Peak Fitting with CasaXPS: A Casa PocketBook. 2010.